

UL-NTZ 11/98

Production of relativistic positronium in collisions of photons and electrons with nuclei and atoms

S. R. Gevorkyan and E. A. Kuraev

Joint Institute of Nuclear Research, Dubna, 141980 Russia

A. Schiller

*Institut für Theoretische Physik and NTZ, Universität Leipzig,
D-04109 Leipzig, Germany*

V. G. Serbo

Novosibirsk State University, Novosibirsk, 630090 Russia

A. V. Tarasov

*Joint Institute of Nuclear Research, Dubna, 141980 Russia
(April 9, 1998)*

Abstract

We consider the production of ultrarelativistic positronium (Ps) in $\gamma A \rightarrow \text{Ps} + A$ and $eA \rightarrow \text{Ps} + eA$ processes where A is an atom or a nucleus with charge Ze . For the photoproduction of para- and ortho-Ps and the electroproduction of para-Ps we obtain the most complete description compared with previous works. It includes high order $Z\alpha$ corrections and polarization effects. The accuracy of the obtained cross sections is determined by omitted terms of the order of the inverse Ps Lorentz factor squared. The studied high order multi-photon electroproduction of ortho-Ps dominates for the collision of electrons with heavy atoms over the bremsstrahlung production from the electron via a virtual photon proposed by Holvik and Olsen. Our results complete and correct the studies of those authors.

PACS numbers: 13.60.-r, 13.85.Qk, 12.20.-m

Typeset using REVTeX

I. INTRODUCTION

The production of relativistic positronium (Ps) opens an attractive possibility to create intensive beams of elementary atoms. It is known that e^+e^- elementary atoms exist in two spin states: parapositronium (para-Ps, singlet state) 1S_0 with lifetime at rest $\tau_0 = 0.123$ ns and orthopositronium (ortho-Ps, triplet state) 3S_1 with $\tau_0 = 0.14$ μ s. The relativistic Ps with lifetime $\tau = \gamma_{\text{Ps}}\tau_0$ (where γ_{Ps} is its Lorentz factor) can be detected far from its creation point which is quite useful from the experimental point of view.

The main motivations to study the positronium production can be summarized as follows: (i) It is the simplest hydrogen-like atom which is very convenient for testing fundamental properties of nature such as the CPT-theorem (see review [1]); (ii) Up to now there is an essential difference between experimental measurements and theoretical calculations of the ortho-Ps width [2]; (iii) Finally, the relativistic Ps has an unusual large transparency in thin layers (see Refs. [3] and literature therein), in QCD a similar property is called color transparency.

In this paper we consider both the Ps production in the collision of high energy photons and electrons with nuclei or atoms A of charge Ze (Figs. 1 and 2):

$$\gamma A \rightarrow \text{Ps} + A, \quad eA \rightarrow \text{Ps} + eA. \quad (1.1)$$

Due to charge parity conservation, the number of exchanged photons between the projectile photon and the target nucleus has to be odd or even for the production of para-Ps or ortho-Ps, respectively.

Let us briefly summarize the present status of calculating the photo- and electroproduction of relativistic positronium. The photoproduction of para-Ps was calculated in main logarithmic approximation in [4] and more precisely in [5]. In both papers effects of high order corrections in the parameter ν

$$\nu = Z\alpha = Z\frac{e^2}{4\pi} \approx Z/137 \quad (1.2)$$

have not been taken into account. In (1.2) Ze denotes the nucleus charge. However, the parameter ν is of the order of 1 for heavy nuclei and, therefore, the whole series in ν has to be summed. These ν effects were considered for para- and ortho-Ps photoproduction in [6], but only for total cross sections with complete screening. Polarization effects of the photon projectile and azimuthal asymmetries in the Ps distribution have not been studied. The electroproduction of para-Ps was calculated in [4,7,8] without high order ν corrections. The corresponding ortho-Ps was considered in [7,8] where only the bremsstrahlung production of Fig. 3 was examined.

The outline of our paper is as follows: In Sect. II we obtain the most complete description of the para- and ortho-Ps photoproduction on nuclei and atoms taking into account polarization, high order corrections in ν and screening effects of target atoms. First the general matrix elements for the Ps production in virtual photon nucleus scattering is presented. Differential and total cross sections for para- and ortho-Ps photoproduction are calculated in the following subsections. Sect. III is devoted to the electroproduction of relativistic positronium. Our exact results for the para-Ps production are compared with calculations using the equivalent photon approximation and neglecting high order ν contributions. In Sect. III C

we present a new mechanism for electroproduction of ortho-Ps, namely, the multi-photon production (summed over two, four, six, ... exchanged photons) of Fig. 2. We show that it may be more important than the bremsstrahlung mechanism of Fig. 3, and even dominates for heavy atoms. In the final section we summarize our results.

Our main notations are collected in Figs. 1, 2: a photon with 4-momentum q and energy ω or an electron with 4-momentum p_e and energy E_e collides with a nucleus of 4-momentum P , mass M and charge Ze and produces Ps described by 4-momentum p , energy E and polarization 4-vector e . We denote by m_e the electron mass, the mass of the e^+e^- bound state and a convenient abbreviation are given as follows

$$m_{\text{Ps}} \approx 2m_e, \quad \sigma_0 = \pi\nu^2 \frac{\alpha^4}{m_e^2}. \quad (1.3)$$

In the electroproduction of Ps (Fig. 2) we deal with a virtual photon generated by the electron. For this photon we use the notations

$$Q^2 = -q^2 > 0, \quad y = \frac{Q^2}{4m_e^2}, \quad \mu = m_e \sqrt{1+y}. \quad (1.4)$$

Throughout the paper we consider the production of relativistic Ps, that means we consider the energy region

$$\begin{aligned} \omega \approx E \gg 2m_e & \quad \text{for} \quad \gamma A \rightarrow \text{Ps} + A, \\ E_e > \omega \approx E \gg 2m_e & \quad \text{for} \quad eA \rightarrow \text{Ps} + eA. \end{aligned} \quad (1.5)$$

II. PHOTOPRODUCTION OF POSITRIONIUM

A. General matrix element for reaction $\gamma^* A \rightarrow \text{Ps} + A$

In this subsection we assume that the photon q is virtual, $q^2 = -Q^2 < 0$, and obtain formulas which will be useful both for photo- and electroproduction of Ps. Choosing the z axis along the photon momentum, the polarization vector for the transverse photon (T -photon with helicity $\lambda_\gamma = \pm 1$) is

$$e_\gamma = (0, e_{\gamma x}, e_{\gamma y}, 0).$$

Taking into account gauge invariance, the polarization vector for the scalar photon (S -photon with helicity $\lambda_\gamma = 0$) can be chosen in the form

$$e_S = \frac{2\sqrt{Q^2}}{s} p_2, \quad p_2 = P - \frac{M^2}{s} q, \quad s = 2qP = 2\omega M.$$

In what follows, we calculate all distributions in an accuracy neglecting only pieces of the order of

$$\frac{(2m_e)^2}{\omega^2}, \quad \frac{\mathbf{p}_\perp^2}{\omega^2}, \quad \frac{Q^2}{\omega^2}. \quad (2.1)$$

Here \mathbf{p}_\perp is the transverse component of the Ps 3-momentum. In this accuracy the momentum transfer squared to the nucleus is given by

$$t = (p - q)^2 = -4\mu^2(\tau + \epsilon^2), \quad \tau = \frac{\mathbf{p}_\perp^2}{4\mu^2}, \quad \epsilon = \frac{\mu}{\omega}. \quad (2.2)$$

The amplitudes of the $\gamma^*A \rightarrow \text{Ps} + \text{A}$ process are obviously closely related to those of the e^+e^- pair production in the field of a heavy nucleus (for equal electron and positron momenta $\mathbf{p}_+ = \mathbf{p}_- = \mathbf{p}/2$). For the latter amplitudes we use the convenient form which was recently obtained in [9]:

$$M(\gamma_T^*A \rightarrow e^+e^-A) = -\frac{Z(4\pi\alpha)^{3/2}}{\mu^3} \bar{u}\hat{p}_2 \left[(\mathbf{n}\mathbf{e}_\gamma + \hat{n}\hat{e}_\gamma) \Phi_s + i\nu \frac{2m_e}{\mu} \hat{e}_\gamma \Phi_t \right] v, \quad (2.3)$$

$$M(\gamma_S^*A \rightarrow e^+e^-A) = \frac{Z(4\pi\alpha)^{3/2}}{\mu^3} i\nu \frac{\sqrt{Q^2}}{\mu} \Phi_t \bar{u}\hat{p}_2 v. \quad (2.4)$$

Here u and v are the spinors of the produced pair of electron and positron, furthermore the 4-unit vector n is defined as

$$n = (0, \mathbf{n}, 0), \quad \mathbf{n} = \frac{\mathbf{p}_\perp}{|\mathbf{p}_\perp|}.$$

The functions Φ_s and Φ_t are given with the help of the Gauss hypergeometric function $F(a, b; c; z)$:

$$\Phi_s \equiv \Phi_s(\tau, \nu, \epsilon) = \frac{\sqrt{\tau}}{(\tau + \epsilon^2)(1 + \tau)} F(i\nu, -i\nu; 1; z) \frac{\pi\nu}{\sinh \pi\nu}, \quad (2.5)$$

$$\Phi_t \equiv \Phi_t(\tau, \nu) = \frac{1 - \tau}{(1 + \tau)^3} F(1 + i\nu, 1 - i\nu; 2; z) \frac{\pi\nu}{\sinh \pi\nu}, \quad (2.6)$$

$$z = \left(\frac{1 - \tau}{1 + \tau} \right)^2. \quad (2.7)$$

Let us briefly mention some main properties of these functions:

$$\begin{aligned} \Phi_s &\rightarrow \frac{\sqrt{\tau}}{(\tau + \epsilon^2)(1 + \tau)}, \quad \Phi_t \rightarrow \frac{1}{1 - \tau^2} \ln \frac{(1 + \tau)^2}{4\tau} \quad \text{at } \nu \rightarrow 0, \\ \Phi_s &\rightarrow \frac{\sqrt{\tau}}{(\tau + \epsilon^2)}, \quad \Phi_t \rightarrow \ln \frac{1}{4\tau} - 2f(\nu) \quad \text{at } \tau \rightarrow 0, \\ \Phi_s &\rightarrow \frac{1}{2} \frac{\pi\nu}{\sinh \pi\nu}, \quad \Phi_t \rightarrow \frac{1}{8}(1 - \tau) \frac{\pi\nu}{\sinh \pi\nu} \quad \text{at } \tau \rightarrow 1, \\ \Phi_s &\rightarrow \frac{1}{\tau^{3/2}}, \quad \Phi_t \rightarrow -\frac{1}{\tau^2} \left[\ln \frac{\tau}{4} - 2f(\nu) \right] \quad \text{at } \tau \rightarrow \infty. \end{aligned} \quad (2.8)$$

The function $f(\nu)$ is well known (see Eq. (95,19) in [10])

$$f(\nu) = \nu^2 \sum_{n=1}^{\infty} \frac{1}{n(n^2 + \nu^2)}. \quad (2.9)$$

For small ν values it behaves as $f(\nu) \approx \zeta(3) \nu^2$ with the Riemann zeta function

$$\zeta(3) = \sum_{n=1}^{\infty} \frac{1}{n^3} = 1.2021. \quad (2.10)$$

As next step the spinors of the electron and positron $\bar{u} \dots v$ are substituted by the wave function of positronium in quantum state n at the origin $\psi(0) = (m_e \alpha)^{3/2} / \sqrt{8\pi n^3}$ according to the rule (see, for example, [11]):

$$\bar{u} \dots v \rightarrow \frac{m_e \alpha^{3/2}}{\sqrt{4\pi n^3}} \frac{1}{4} \text{Tr} [\dots (\hat{p} + m_{\text{Ps}}) \Gamma]. \quad (2.11)$$

Here Γ is a projection operator to be chosen as $\Gamma = i\gamma^5$ for the para-Ps and $\Gamma = \hat{e}^*$ for the ortho-Ps state.

Now the amplitudes of Ps production by T - or S -photons can be obtained using (2.3), (2.4) and (2.11). The para-Ps is produced only by transverse photons

$$M(\gamma_T^* A \rightarrow n^1S_0 + A) = \frac{2\pi Z\alpha^3}{n^{3/2}} \frac{s}{m_e^2(1+y)^{3/2}} (\mathbf{e}_\gamma \times \mathbf{n}) \cdot \frac{\mathbf{q}}{\omega} \Phi_s, \quad (2.12)$$

$$M(\gamma_S^* A \rightarrow n^1S_0 + A) = 0. \quad (2.13)$$

For the ortho-Ps production there are two possibilities: The transversely polarized ortho-Ps (with helicity $\lambda = \pm 1$) arises from transverse photons only

$$M(\gamma_T^* A \rightarrow n^3S_1 + A) = -i \frac{4\pi Z^2 \alpha^4}{n^{3/2}} \frac{s}{m_e^2(1+y)^2} (\mathbf{e}_\gamma \cdot \mathbf{e}^*) \Phi_t, \quad (2.14)$$

while the longitudinally polarized ortho-Ps (with helicity $\lambda = 0$) is produced by scalar photons

$$M(\gamma_S^* A \rightarrow n^3S_1 + A) = i \frac{\sqrt{Q^2}}{2m_e} \frac{4\pi Z^2 \alpha^4}{n^{3/2}} \frac{s}{m_e^2(1+y)^2} \Phi_t. \quad (2.15)$$

From (2.14) and (2.15) we observe that helicity is conserved in the $\gamma \rightarrow$ ortho-Ps transition, i. e. $\lambda_\gamma = \lambda$. We also notice that both amplitudes (2.14), (2.15) do not depend on the azimuthal angle of ortho-Ps.

In the following parts of this section we study the production of positronium by real photons. Therefore, in all expressions we have to choose (see (1.4)) $Q^2 = 0$, $y = 0$.

B. Photoproduction of para-Ps

The differential cross section of para-Ps production on nuclei can be obtained using the amplitude (2.12) at $Q^2 = 0$

$$d\sigma_{\text{singlet}} = \frac{\sigma_0}{n^3} |\mathbf{e}_\gamma \times \mathbf{n}|^2 \Phi_s^2 d\tau \frac{d\varphi}{2\pi} \quad (2.16)$$

where φ is the azimuthal angle of Ps. To describe the polarization degree of the initial photon in general, it is convenient to use Stokes parameters $\xi_{1,2,3}$. In that case (2.16) transforms to

$$d\sigma_{\text{singlet}} = \frac{\sigma_0}{2n^3} [1 + \xi_1 \sin 2\varphi - \xi_3 \cos 2\varphi] \Phi_s^2 d\tau \frac{d\varphi}{2\pi}. \quad (2.17)$$

We see that this cross section does not depend on ξ_2 , i.e. on the circular polarization of photon. Furthermore, the scattering plane is mainly orthogonal to the direction of the linear polarization of the photon. For $\xi_i \rightarrow 0$ and $\nu \rightarrow 0$ the result (2.17) coincides with that obtained in [5].

The dependence of cross section (2.17) on the Ps polar angle θ is completely described by the function $\Phi_s^2(\tau, \nu, \epsilon)$ since in our case

$$\tau = \left(\frac{\omega\theta}{2m_e} \right)^2. \quad (2.18)$$

According to (2.8) the function $\Phi_s(\tau, \nu, \epsilon)$ depends on ν only in the region $\tau \sim 1$, whereas for $\tau \ll 1$ and $\tau \gg 1$ the angular behavior of cross section (2.17) has an universal (independent on ν) character. In particular, in the region of very small angles

$$\frac{m_e^2}{\omega^2} \ll \theta \ll \frac{m_e}{\omega} \quad (2.19)$$

the differential cross section has a very simple form

$$d\sigma_{\text{singlet}} = \frac{\sigma_0}{n^3} \frac{d\theta}{\theta}.$$

The total cross section is obtained from (2.17) by integrating over φ and τ and by summing over all n^1S_0 quantum states:

$$\sigma_{\text{singlet}} = \sigma_0 \zeta(3) \left[\ln \frac{\omega}{m_e} - 1 - C(\nu) \right], \quad (2.20)$$

$$\begin{aligned} C(\nu) &= \frac{1}{2} \int_0^\infty \left\{ 1 - \left[F(i\nu, -i\nu; 1; z) \frac{\pi\nu}{\sinh \pi\nu} \right]^2 \right\} \frac{d\tau}{\tau(1+\tau)^2} \\ &= \frac{1}{4} \int_0^1 \left\{ 1 - \left[F(i\nu, -i\nu; 1; z) \frac{\pi\nu}{\sinh \pi\nu} \right]^2 \right\} \frac{(1+z)dz}{(1-z)\sqrt{z}}. \end{aligned} \quad (2.21)$$

The function $C(\nu)$ is presented in Fig. 4, at small ν it is approximated by

$$C(\nu) = \left[\frac{7}{2} \zeta(3) - 4 + 4 \ln 2 \right] \nu^2 \approx 2.9798 \nu^2. \quad (2.22)$$

Note that the large logarithmic term $\ln(\omega/m_e)$ in cross section (2.20) arises just from the region of small angles (2.19). Therefore, this region determines the characteristic polar angle of para-Ps production $\theta_{\text{char}}^{1S_0}$.

Up to now we have considered the photoproduction of positronium on nuclei. Let us briefly discuss the photoproduction on atoms where a possible atomic screening has to be taken into account. This can be done by inserting a factor $(1 - F(t))$ in the amplitude (2.12) (and $(1 - F(t))^2$ in the cross sections (2.16) or (2.17)) where $F(t)$ is the atomic form factor and t is given in (2.2). As a result, we obtain the total cross section for photoproduction of para-Ps on atoms:

$$\sigma_{\text{singlet}} = \sigma_0 \zeta(3) [J - C(\nu)], \quad J = \frac{1}{2} \int_0^\infty \frac{\tau [1 - F(t)]^2}{(\tau + \epsilon^2)^2 (1 + \tau)^2} d\tau. \quad (2.23)$$

If we use a simplified Thomas-Fermi-Moliére form factor

$$F(t) = \frac{1}{1 - (t/\Lambda^2)}, \quad \Lambda = \frac{Z^{1/3}}{111} m_e, \quad (2.24)$$

we obtain in accuracy (2.1)

$$J = -\frac{1}{2} \ln \left[\left(\frac{m_e}{\omega} \right)^2 + \left(\frac{Z^{1/3}}{222} \right)^2 \right] - 1. \quad (2.25)$$

At not very high energies

$$2m_e \ll \omega \ll \frac{2m_e^2}{\Lambda} = \frac{222}{Z^{1/3}} m_e \quad (2.26)$$

the screening effects are negligible in J and the previous result for the nucleus target (2.20) remains valid. For high enough energies

$$\omega \gg \frac{222}{Z^{1/3}} m_e, \quad (2.27)$$

there is complete screening and the total cross section takes the form

$$\sigma_{\text{singlet}} = \sigma_0 \zeta(3) \left[\ln \frac{222}{Z^{1/3}} - 1 - C(\nu) \right] \quad (2.28)$$

which coincides with the result obtained in [6].

C. Photoproduction of ortho-Ps

The differential cross section of ortho-Ps production on nuclei can be obtained using the amplitude (2.14). For polarized photons it is given by

$$d\sigma_{\text{triplet}} = 4\nu^2 \frac{\sigma_0}{n^3} |\mathbf{e}_\gamma \cdot \mathbf{e}^*|^2 \Phi_t^2 d\tau, \quad (2.29)$$

for unpolarized photons we have

$$d\sigma_{\text{triplet}} = 4\nu^2 \frac{\sigma_0}{n^3} \Phi_t^2 d\tau. \quad (2.30)$$

The dependence of this cross section on τ (and therefore on the polar angle of positronium θ , see (2.18)) is given by the function Φ_t^2 , it is presented in Fig. 5. $d\sigma_{\text{triplet}}/d\tau$ vanishes for all values of ν as $(1 - \tau)^2$ at $\tau \rightarrow 1$ (see (2.8)).

Comparing (2.17) and (2.30) we conclude that the angular distributions of ortho-Ps production is considerably wider than that of para-Ps production. Indeed, the typical value of τ for ortho-Ps production is of the order of 0.1 which corresponds to a characteristic emission angle

$$\theta_{\text{char}}^{3S_1} \sim \frac{m_e}{\omega}, \quad (2.31)$$

while for para-Ps production on nuclei the region of very small angles (2.19) gives the main contribution to the cross section.

The total cross section, obtained from (2.30), is independent on the energy of the initial photon:

$$\sigma_{\text{triplet}} = 4(Z\alpha)^2 \sigma_0 \zeta(3) B(\nu). \quad (2.32)$$

Here the function $B(\nu)$ is

$$B(\nu) = \int_0^\infty \Phi_t^2(\tau, \nu) d\tau = \left(\frac{\pi\nu}{\sinh \pi\nu} \right)^2 \frac{1}{8} \int_0^1 \sqrt{z}(1+z) [F(1 + i\nu, 1 - i\nu; 2; z)]^2 dz, \quad (2.33)$$

its dependence on Z is shown in Fig. 6. At small $\nu \ll 1$ this function behaves as [6]:

$$B(\nu) = 2 - 2 \ln 2 - \left[8(2 - \ln 2)^2 - \frac{2}{3}\pi^2 - 5\zeta(3) \right] \nu^2 \approx 0.6137 - 1.0729\nu^2. \quad (2.34)$$

The obtained results for the photoproduction of ortho-Ps on nuclei are also valid for the production on atoms. Indeed, the typical value of $\tau^{3S_1} \sim 0.1$ for photoproduction on nuclei is much larger than the characteristic value

$$\tau_{\text{screen}} \sim \left(\frac{\Lambda}{2m_e} \right)^2 = \left(\frac{Z^{1/3}}{222} \right)^2$$

for which we should take into account the atomic form factor (see (2.24)).

At the end of this section let us compare the photoproduction of ortho- and para-Ps on atoms. For energies $\omega \gg 222m_e/Z^{1/3}$ the ratio

$$\frac{\sigma_{\text{triplet}}}{\sigma_{\text{singlet}}} = \frac{4\nu^2 B(\nu)}{\ln(222/Z^{1/3}) - 1 - C(\nu)} \quad (2.35)$$

is presented as function of the nucleus charge number Z in Fig. 7. Some particularly interesting values are 28.5 %, 23.5 % and 1.51 % for U, Pb and Ca, respectively.

III. ELECTROPRODUCTION OF POSITRONIUM

A. General expressions for reaction $eA \rightarrow \text{Ps} + eA$

It is well known that the cross section for the electroproduction of Fig. 2 can be exactly written in terms of two structure functions or two cross sections $\sigma_T(\omega, Q^2)$ and $\sigma_S(\omega, Q^2)$ for the processes $\gamma_T^* A \rightarrow \text{Ps} + A$ and $\gamma_S^* A \rightarrow \text{Ps} + A$:

$$d\sigma(eA \rightarrow \text{Ps} + eA) = \sigma_T(\omega, Q^2) dn_T(\omega, Q^2) + \sigma_S(\omega, Q^2) dn_S(\omega, Q^2). \quad (3.1)$$

Here the coefficients dn_T and dn_S can be called the number of transverse and scalar virtual photons, respectively. Using the amplitudes (2.12)-(2.15) for the corresponding processes the cross sections σ_T and σ_S are calculable for virtual photon energies squared

$$\omega^2 \gg (2m_e)^2, Q^2 \quad (3.2)$$

with accuracy (2.1). In the same region and with the same accuracy the quantities dn_T and dn_S are (see, for example, Sect. 6 in review [12])

$$dn_T = \frac{\alpha}{\pi} N \left(\frac{\omega}{E_e}, \frac{Q^2}{4m_e^2} \right) \frac{d\omega}{\omega} \frac{dQ^2}{Q^2}, \quad N(x, y) = 1 - x + \frac{1}{2}x^2 - \frac{x^2}{4y}, \quad (3.3)$$

$$dn_S = \frac{\alpha}{\pi} \left(1 - \frac{\omega}{E_e} \right) \frac{d\omega}{\omega} \frac{dQ^2}{Q^2}. \quad (3.4)$$

The variable y is defined in (1.4). Since the energy E of the positronium almost coincides with that of the virtual photon, the energy fraction transferred from the electron to Ps is

$$x = \frac{E}{E_e} = \frac{\omega}{E_e}. \quad (3.5)$$

B. Electroproduction of para-Ps

The cross sections σ_T and σ_S for para-Ps production are obtained using (2.12), (2.13) and repeating the calculations of Sect. II B with $Q^2 > 0$. This leads to

$$d\sigma_T = \frac{\sigma_0}{2n^3(1+y)^2} \Phi_s^2 d\tau, \quad d\sigma_S = 0, \quad (3.6)$$

(with τ defined in (2.2)) and to the integrated cross sections

$$\sigma_T = \frac{\sigma_0}{(1+y)^2} \zeta(3) [L - 1 - C(\nu)], \quad \sigma_S = 0. \quad (3.7)$$

Here for the electroproduction on nuclei (compare (2.17), (2.20))

$$L = \ln \frac{\omega}{m_e} - \frac{1}{2} \ln(1+y) \quad (3.8)$$

and on atoms (compare (2.23), (2.25))

$$L = -\frac{1}{2} \ln \left[\left(\frac{m_e}{\omega} \right)^2 (1+y) + \left(\frac{\Lambda}{2m_e} \right)^2 \frac{1}{(1+y)} \right]. \quad (3.9)$$

Using (3.1)-(3.9) we are able to obtain the energy-angular and energy distributions of relativistic Ps. In particular, the spectrum of para-Ps is

$$d\sigma(eA \rightarrow {}^1S_0 + eA) = \frac{\alpha}{\pi} \sigma_0 \zeta(3) F_s(x) \frac{dx}{x}, \quad (3.10)$$

$$F_s(x) = \int_{y_m}^{\infty} \frac{[L - 1 - C(\nu)]}{(1+y)^2} N(x, y) \frac{dy}{y}, \quad y_m = \frac{x^2}{4(1-x)}$$

(Since the cross section rapidly decreases above $y \approx 1$, the upper integration limit can be extended to infinity.).

For the electroproduction on nuclei the y integration is easily performed and we obtain

$$F_s(x) = f_1(x) \left[\ln \frac{x E_e}{m_e} - 1 - C(\nu) \right] - f_2(x). \quad (3.11)$$

The functions $f_1(x)$ and $f_2(x)$ can be presented as follows:

$$f_1(x) = 2(1-x+x^2) \ln \frac{2-x}{x} - \frac{4(1-x)}{(2-x)^2} (2-2x+x^2),$$

$$f_2(x) = (1-x+x^2) \left[\frac{\pi^2}{12} - \frac{2(1-x)}{(2-x)^2} - \frac{1}{2} \text{Li}_2 \left(\frac{x^2}{(2-x)^2} \right) \right] + \frac{x^2}{4} \left(\frac{2(1-x)}{(2-x)^2} + \ln \frac{x}{2-x} \right) - \frac{2(1-x)}{(2-x)^2} (2-2x+x^2) \ln \frac{(2-x)^2}{4(1-x)} \quad (3.12)$$

with the dilogarithm function

$$\text{Li}_2(z) = \int_z^0 \frac{\ln(1-t)}{t} dt.$$

Note that $f_2(x) < f_2(0) = (\pi^2 - 6)/12 = 0.3225$.

The same result (3.11) is valid for electroproduction on atoms at $2m_e \ll x E_e \ll 222m_e/Z^{1/3}$ (no screening). For the case of complete screening ($x E_e \gg 222m_e/Z^{1/3}$) we have

$$F_s(x) = f_1(x) \left[\ln \frac{222}{Z^{1/3}} - 1 - C(\nu) \right] + f_2(x). \quad (3.13)$$

In the important case of small x (i.e. at $2m_e/E_e \ll x \ll 1$) the spectrum is simplified:

$$F_s(x) = \left(2 \ln \frac{2}{x} - 2 \right) \left[\ln \frac{x E_e}{m_e} - 1 - C(\nu) \right] - \frac{\pi^2 - 6}{12} \quad (3.14)$$

for no screening and

$$F_s(x) = \left(2 \ln \frac{2}{x} - 2\right) \left[\ln \frac{222}{Z^{1/3}} - 1 - C(\nu) \right] + \frac{\pi^2 - 6}{12} \quad (3.15)$$

for complete screening. The accuracy of the obtained spectrum is determined by omitting terms of the order of

$$\left(\frac{2m_e}{xE_e} \right)^2. \quad (3.16)$$

It is interesting to compare our spectra (3.10)-(3.15) with that given in [8]

$$F_s^{\text{HO}}(x) = \left(2 \ln \frac{1}{x} - 1\right) \left\{ -\frac{1}{2} \ln \left[\left(\frac{m_e}{xE_e} \right)^2 + \left(\frac{Z^{1/3}}{222} \right)^2 \right] - 1 \right\}. \quad (3.17)$$

The spectrum $F_s^{\text{HO}}(x)$ was obtained neglecting the exact dependence of σ_T on Q^2 and high order ν corrections. As a consequence, the accuracy of (3.17) is only logarithmic (in expressions (3.14)-(3.15) and (3.17) the leading logarithmic terms coincide whereas the next to leading logarithmic terms are different even at $\nu \ll 1$). Therefore, this approximation is not well suited for heavy atoms. For example, in the case of complete screening the spectrum $F_s^{\text{HO}}(x)$ exceeds our spectrum $F_s(x)$ up to approximately 40 % for U and 30 % for Pb in the x region below 0.4.

C. Electroproduction of ortho-Ps

The ortho-Ps production in collisions of electrons with atoms due to the bremsstrahlung mechanism of Fig. 3 was calculated in [7,8]. The principal features of this mechanism are the following: The spectrum of ortho-Ps has a peak in the region of high energy fractions (at $x \approx 1$), the characteristic emission angle of Ps is small

$$\theta_{\text{char}}^{\text{br}} \sim \frac{m_e}{E_e}. \quad (3.18)$$

The total cross section is equal to [8]

$$\sigma_{\text{br}} = \frac{\alpha}{\pi} \sigma_0 \zeta(3) I_{\text{br}} \quad (3.19)$$

where

$$I_{\text{br}} = 0.303 \ln \frac{E_e}{m_e} - 0.542 \quad (3.20)$$

for no screening ($E_e \ll 444m_e/Z^{1/3}$) and

$$I_{\text{br}} = 0.303 \ln \frac{111}{Z^{1/3}} + 0.362 \quad (3.21)$$

for complete screening ($E_e \gg 444m_e/Z^{1/3}$).

In this section we argue that in many respects these results are incomplete or even misleading because in [7,8] the important multi-photon production (MP) of ortho-Ps due

to diagrams of Fig. 2 with even numbers $j = 2, 4, 6, \dots$ of exchanged photons was not considered. Moreover, we find out that MP production is dominant for electron scattering on heavy atoms.

To study the MP production of ortho-Ps, we have to calculate the cross sections σ_T and σ_S for ortho-Ps production (see (3.1)). This is achieved using the corresponding amplitudes (2.14), (2.15) and repeating the calculations of Sect. II C with $Q^2 > 0$. For the cross sections we obtain (compare (2.30), (2.32))

$$d\sigma_T = 4\nu^2 \frac{\sigma_0}{n^3(1+y)^3} \Phi_t^2 d\tau, \quad d\sigma_S = y d\sigma_T, \quad (3.22)$$

$$\sigma_T = 4\nu^2 \frac{\sigma_0}{(1+y)^3} \zeta(3) B(\nu), \quad \sigma_S = y \sigma_T. \quad (3.23)$$

Using these formulas and (3.1) we can again obtain the energy-angular and energy distributions for the triplet state of relativistic positronium. In particular, now the spectrum of ortho-Ps is

$$d\sigma_{\text{MP}} = \frac{4\alpha}{\pi} (Z\alpha)^2 \sigma_0 \zeta(3) B(\nu) F_t(x) \frac{dx}{x}, \quad (3.24)$$

$$F_t(x) = 2 \left(1 - x + \frac{5}{4}x^2\right) \ln \frac{2-x}{x} - \frac{(1-x)}{(2-x)^4} [32(1-x)^2 + 34(1-x)x^2 + 5x^4]. \quad (3.25)$$

The spectrum (function $F_t(x)/x$) is shown in Fig. 8. The result (3.24), (3.25) is valid for collisions of electrons both with nuclei and atoms. The behavior of function $F_t(x)$ at small and large x is the following:

$$F_t(x) = 2 \ln \frac{2}{x} - 2 \quad \text{at } x \ll 1, \quad F_t(x) = \frac{56}{3}(1-x)^3 \quad \text{at } 1-x \ll 1. \quad (3.26)$$

Contrary to the bremsstrahlung spectrum (see Fig. 3 in [8]), the spectrum (3.24) is peaked at small energies of Ps. Therefore, the interference of bremsstrahlung and MP production should be very small.

Taking into account (2.31) and (3.5), we conclude that the characteristic angle for MP production of ortho-Ps is

$$\theta_{\text{char}}^{\text{MP}} \sim \frac{m_e}{xE_e} \quad (3.27)$$

which is much larger than (3.18). In other words, the angular distribution of MP production is considerably wider than that of the bremsstrahlung reaction.

In this section the spectra for relativistic positronium in electroproduction have been calculated with the high accuracy (3.16). This accuracy cannot be achieved for the total cross sections in the scheme used here by the following reasons: The spectrum has to be integrated over the whole kinematic region in x including that of the threshold $x \sim 2m_e/E_e$. But near the threshold the accuracy of our calculated spectra becomes only logarithmic. Furthermore, in this region Ps is not a relativistic particle and, therefore, its detection

is difficult. However, if we are interested to find the total cross section with logarithmic accuracy, we can integrate the spectra in the whole region

$$x_m = \frac{2m_e}{E_e} \leq x \leq 1. \quad (3.28)$$

Having in mind this restriction, we find for the total cross section of MP production

$$\sigma_{\text{MP}} \approx \frac{4\alpha}{\pi} (Z\alpha)^2 \sigma_0 \zeta(3) B(\nu) I_{\text{MP}}, \quad (3.29)$$

$$I_{\text{MP}} = \int_{x_m}^1 F_t(x) \frac{dx}{x} \approx \left(\ln \frac{E_e}{m_e} \right)^2 - 2 \ln \frac{E_e}{m_e} - c, \quad c = \frac{\pi^2}{6} - \frac{5}{4} = 0.3949.$$

Note that this multi-photon cross section increases with the energy of the projectile electron as $[\ln(E_e/m_e)]^2$ while the cross section for the bremsstrahlung production on atoms is constant at high energies (see (3.21)). The dependence of the cross section ratio

$$\frac{\sigma_{\text{MP}}}{\sigma_{\text{br}}} = 4\nu^2 B(\nu) \frac{I_{\text{MP}}}{I_{\text{br}}} \quad (3.30)$$

on the initial electron energy E_e is presented in Fig. 9 for different values of Z . From that picture it can be seen that the MP production is the dominant production mechanism of orthopositronium for atoms with nucleus charge number $Z > 20$.

IV. SUMMARY

In this paper we have presented an almost complete description of the production of relativistic positronium in high energy photon and electron collisions with nuclei and atoms. The high accuracy of our results is restricted by neglecting terms of the order of the inverse Ps Lorentz factor squared $(2m_e/E)^2$.

The matrix elements of the virtual photon nucleus scattering to produce both para- and ortho-Ps are given in (2.12)-(2.15) including polarizations of the initial photon and the positronium and summed high order $Z\alpha$ corrections. The singlet positronium state can be produced only by transversely polarized initial photons, the transition amplitude depends on the azimuthal angle of 1S_0 . The amplitude for scalar virtual photons to para-Ps is zero. The transitions from the initial virtual transverse and scalar photon to the triplet state are accompanied with helicity conservation $\lambda_\gamma = \lambda$, the amplitudes do not depend on the azimuthal angle of ortho-Ps.

These results are used to discuss both photo- and electroproduction of Ps. Various distributions and total cross sections are calculated and compared to previous results. The screening effects are estimated analytically using a Thomas-Fermi-Moli  re atomic form factor.

For the photoproduction of relativistic positronium we have found that the polar angular distribution of ortho-Ps is considerably wider than that of para-Ps. The high order $Z\alpha$ effects decreases the ortho-Ps photoproduction cross section by 3.61 % for Ca, 40.5 % for Pb and 46.5 % for U nuclei. The ratio of the total cross sections for the triplet to singlet state at

higher energies $\omega \gg 222m_e/Z^{1/3}$ in the $\gamma A \rightarrow {}^3S_1 + A$ process raises with the nucleus charge number from 1.51 % for Ca, 23.5 % for Pb to 28.5 % for U targets.

In the para-Ps electroproduction the virtuality of the photons arising from the electron projectile and the effects of heavy nuclei are quite important. As an example, the spectrum [8] estimated in an equivalent photon approximation and with neglected high order $Z\alpha$ effects exceeds the correctly calculated result up to 30 % for Pb and 40 % for U in a wide range of the energy fraction transferred from the electron to Ps.

Finally we have proposed a new multi-photon mechanism for the production of ortho-Ps in the reaction $eA \rightarrow {}^3S_1 + eA$ which has to be taken into account besides the bremsstrahlung production discussed by Holvik and Olsen. Due to a completely different angular and energy distribution of MP its interference with the bremsstrahlung reaction is expected to be small. This new mechanism is dominant for electron scattering on heavy atoms. Therefore, our results complete and correct those earlier studies.

At the end we would like to note that our results cannot be straightforwardly transformed to the production of $\mu^+\mu^-$ elementary atom called dimuonium (DM). For the photo- and electroproduction of DM a new important phenomenon takes place, namely, the restriction of the transverse momenta $k_{1\perp}, \dots, k_{j\perp}$ for the exchanged photons in Figs. 1, 2. This restriction arises due to the nucleus form factor at the level $\lesssim 1/r_A \ll m_\mu$ where r_A is the electromagnetic radius of the nucleus. As a result, the effective parameter of the perturbation theory becomes small $\sim \nu^2/(r_A m_\mu)^2 \lesssim 0.03$, contrary to the Ps case. A detailed study of DM production will be presented in [13].

ACKNOWLEDGMENTS

We are grateful to R. Faustov, I. Ginzburg, I. Khriplovich, I. Meshkov and L. Nemenov for useful discussions and to A. Arbuzov, O. Krehl and B. Shaikhutdenov for help. The work of S.R.G. and E.A.K. was supported by INTAS grant 93-239 ext, the work of V.G.S is supported by Volkswagen Stiftung (Az. No.1/72 302) and by Russian Foundation for Basic Research (grant 96-02-19114).

REFERENCES

- [1] I. N. Meshkov, *Elem. Particles and Nuclei* **28**, 495 (1997).
- [2] I. B. Khriplovich, A. I. Milstein, Novosibirsk preprint Budker-INP 96-49 (1996).
- [3] L. L. Nemenov, *Yad. Fiz.* **51**, 444 (1990), [Sov. J. Nucl. Phys. **51** 284 (1990)]; V. L. Lyuboshitz, M. I. Podgoretsky, *ZhETF* **81**, 1556 (1981).
- [4] G. V. Meledin, V. G. Serbo, A. K. Slivkov, *Pis'ma ZhETF* **13**, 98 (1971) [JETP Lett. **13**, 68 (1971)].
- [5] H. A. Olsen, *Phys. Rev.* **D33**, 2033 (1986).
- [6] A. V. Tarasov, I. V. Christova, Dubna preprint JINR P2-91-4, (1991).
- [7] A. A. Akhundov, D. Yu. Bardin, L. L. Nemenov, *Yad.Fiz.* **27**, 1542 (1978).
- [8] E. Holvik, H. A. Olsen, *Phys. Rev.* **D35**, 2124 (1987).
- [9] D. Ivanov, K. Melnikov, *Phys. Rev.* **D57**, 4025 (1998).
- [10] V. B. Berestetskii, E. M. Lifshitz, L. B. Pitaevskii, *Quantum Electrodynamics* (Nauka, Moscow, 1989).
- [11] V. A. Novikov et al., *Phys. Rep.* **41C**, 1 (1978).
- [12] V. M. Budnev, I. F. Ginzburg, G. V. Meledin, V. G. Serbo, *Phys. Rep.* **C15**, 181 (1975).
- [13] I. F. Ginzburg, V. D. Jentschura, S. G. Karshenboim, F. Krauss, V. G. Serbo, G. Soff (in preparation).

FIGURES

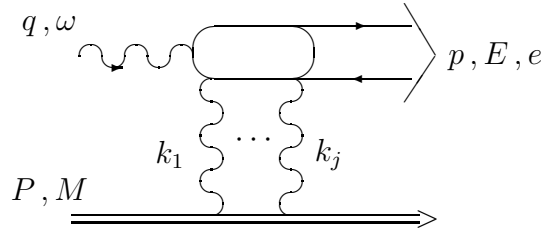


FIG. 1. Photoproduction of Ps on nucleus with odd (even) number j of exchanged photons for para-Ps (ortho-Ps).

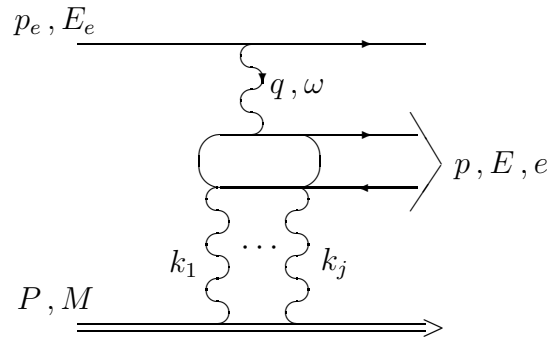


FIG. 2. Electroproduction of Ps on nucleus.

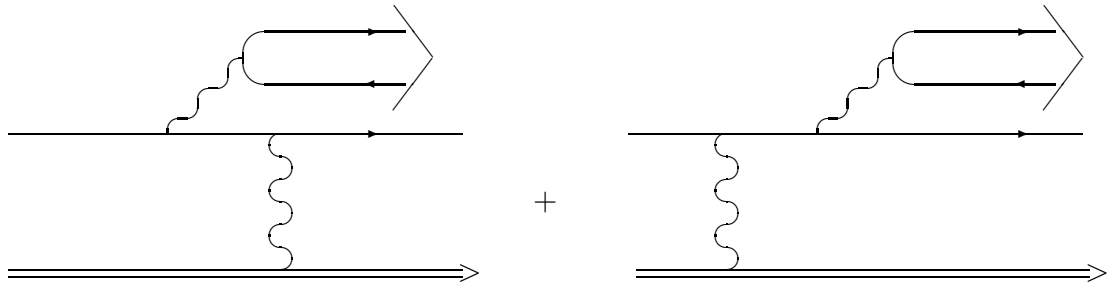


FIG. 3. Bremsstrahlung production of ortho-Ps on nucleus.

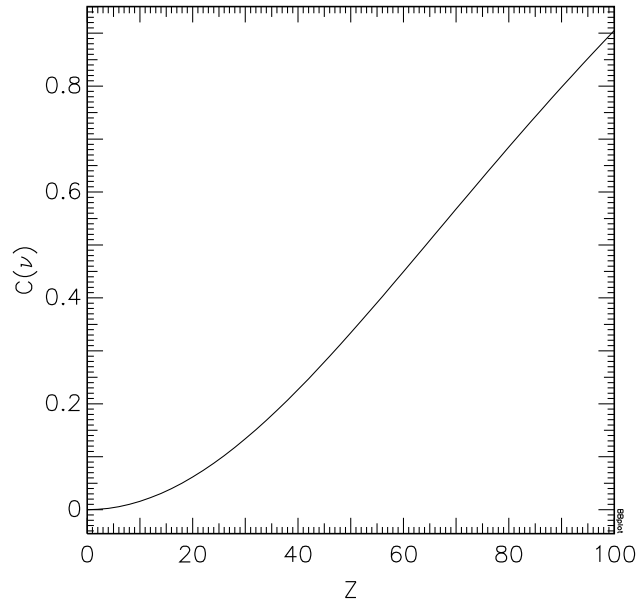


FIG. 4. Function $C(\nu)$ (2.21) vs. nucleus charge number Z .

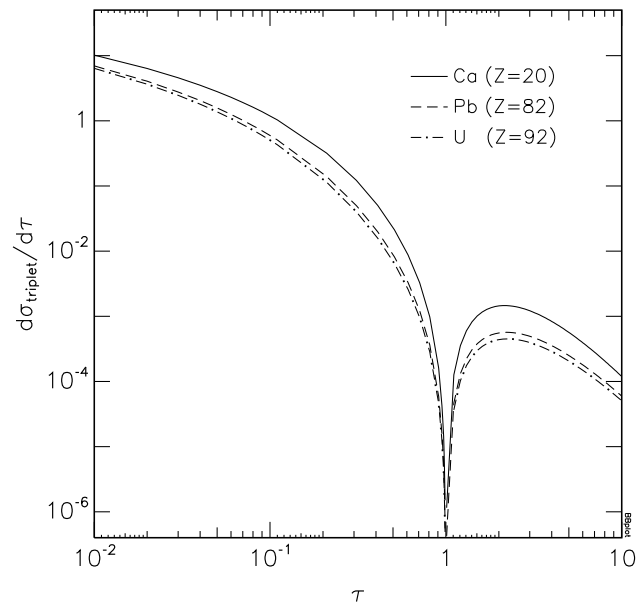


FIG. 5. Differential cross section $d\sigma_{\text{triplet}}/d\tau$ in units $4\nu^2\sigma_0/n^3$.

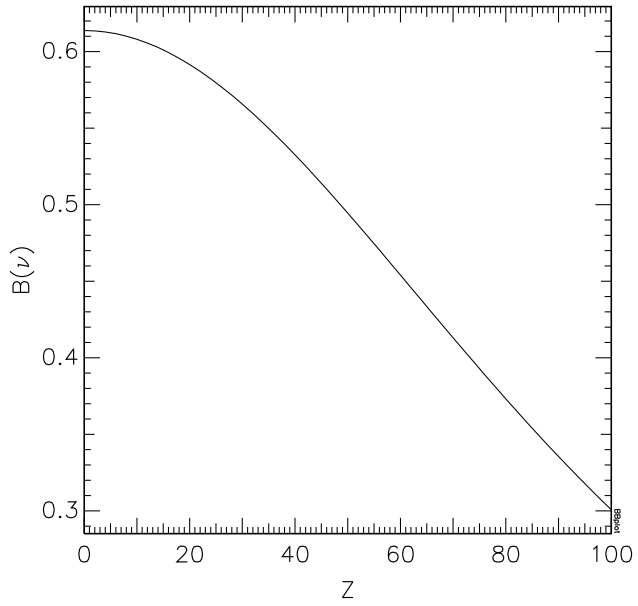


FIG. 6. Function $B(\nu)$ ((2.33)) vs. Z .

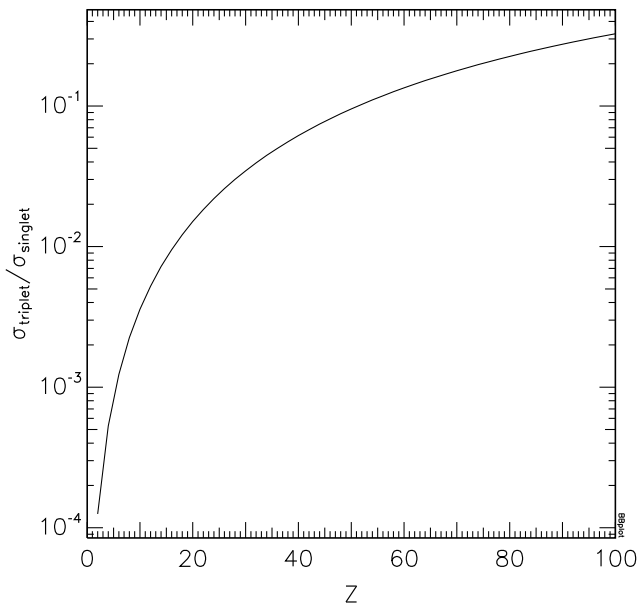


FIG. 7. Ratio $\sigma_{\text{triplet}}/\sigma_{\text{singlet}}$ in photoproduction on atoms at larger energies as function of Z .

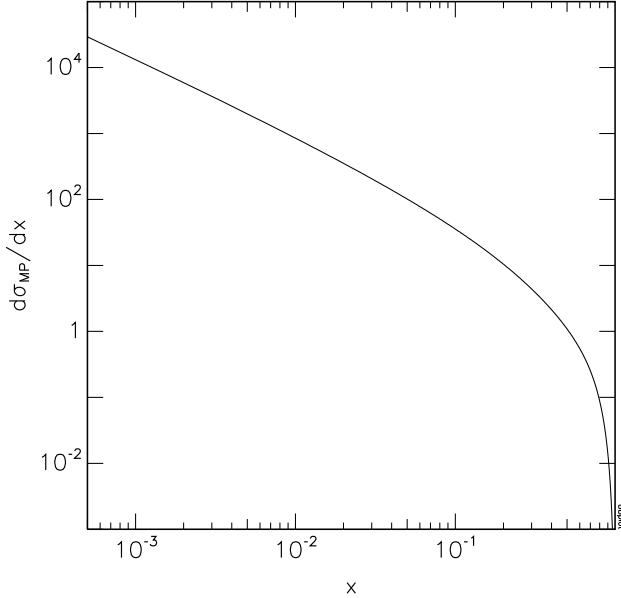


FIG. 8. Ortho-Ps spectrum in electroproduction in units of $(4\alpha/\pi)\sigma_0 \zeta(3) \nu^2 B(\nu)$ due to multi-photon mechanism of Fig. 2.

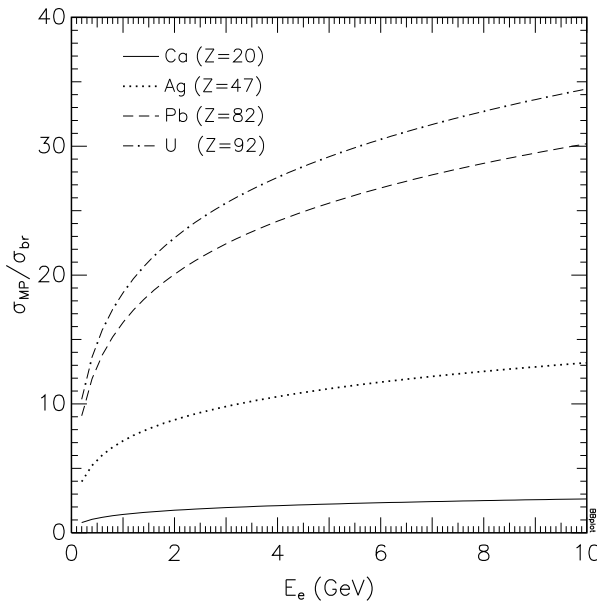


FIG. 9. Ratio σ_{MP}/σ_{br} of multi-photon (Fig. 2) to bremsstrahlung cross section (Fig. 3) as function of the electron beam energy E_e .